Journal of Harbin Engineering University
ISSN: 1006-7043

Vol 45 No. 4
April 2024

Effect of Corner Modifications on the Drag Coefficient of a Square Cylinder

T. Yane[1] , N. Subaschandar[2]
[1]Department of Mathematics, University of Botswana, Gaborone, Botswana, Email: yanet@ub.ac.bw
[2]Department of Mathematics and Statistical Sciences, Botswana International University of Science and Technology, Palapye, Botswana. Email: raos@biust.ac.bw

Abstract: In this study, the coefficient of drag of several variations of square cylinder, with and without corner modifications, in a two-dimensional turbulent fluid flow was examined. A square cylinder with sharp edges, square cylinders with rounded corners, and square cylinders with chamfered corners were the configurations examined. Impact of modifying only leading corners and only trailing corners on the drag coefficient was studied. Corner radius and chamfer length were gradually modified between 0 to 0.28D where D is the side length of the unmodified square cylinder. Using Computational Fluid Dynamics technique and EASYCFD software, the drag coefficient for all configurations was calculated. The square cylinder with corner round radius of 0.24D had the lowest drag coefficient, which was followed by the square cylinder with a corner chamfer length of 0.24D, while the unmodified square cylinder had the highest drag coefficient. This paper sheds some important light on the understanding of the impact of corner shape on the drag force experienced by the tall buildings, marine structures, road, and air-borne vehicles.

Keywords: Square cylinder, drag coefficient, turbulence models, corner modification.

1. Introduction

The fluid flow around buildings is becoming progressively significant because of using lightweight supplies used in the construction. It is very difficult to design land or ocean buildings and ships without a clear grasp of flow-generated mechanical forces, flow-induced mass and heat transfer, vortex shedding phenomenon, fluid-structure interaction. . . etc. In the domain of marine engineering, floating ocean constructions are often subjected to ocean current flow and extreme wind conditions at high ranges of Reynolds number (Re). They are exposed to the hydrodynamic and aerodynamic forces related to the turbulent ocean currents. The correct prediction of the fluid flow characteristics and the resultant forces on physical components of different cross-sectional forms are vital parts in the design and function of seaward systems. It is well-known that the fluid flow separation plays a very important part in changing the fluid flow past bluff bodies. In the case of a square cylinder, the fluid flow at Reynolds number(Re) < 95 and Reynolds number(Re) > 95 is compelled to separate from the leading and trailing corners of the cylinder, respectively, because of the geometrical discontinuity [1]. However, on a circular cylinder, the fluid flow separation happens naturally because of an adverse pressure gradient on the cylinder's curved surface and creates a relatively thinner wake yielding a smaller drag force compared to the square cylinders. The drag coefficient of a square cylinder with sharp corners in a high Re flow is about 2.2 while that of a circular cylinder is about 1.2[2]. Although broadly handled in engineering, the circular cylinder may not be the optimum shape with minimum drag, which suggests that adjustment of the square cylinder sharp corners may help in reducing the drag force further. The adjustment can be rounding, chamfering, recessing, or cutting the corners. Research reports [3,4] provide excellent reviews of impact of such modifications on the flow past bluff bodies.

Aerodynamic alteration of bluff objects like square cylinder and circular cylinder has drawn extensive attention due to its practical significance. Studies are reported in the areas of decreasing wind-forced vibration of engineering constructions, improving the vibration of wind energy harvesters and, also, because of many interesting phenomena including fluid flow instability, vortex shedding, fluid flow separation, recirculation, flow transition etc. Most

of these studies are concentrated on aerodynamic alterations to reduce wind-forced vibration for safeguarding structural security [5-7]. The conventional approaches to achieve this objective include jet flow control [8], slotting corners [9], fitting solid or vented fins in the corners [9,10], chamfering corners [11], rounding corners [12,13], recessing corners [14-16]. The study reported in [9] observed that using solid and vented fins on the sharp corners of a square tall building had significant impact on both along wind and crosswind activities. The corner fins may be a choice for decreasing wind forces on bridge pillars if it is designed properly. In this study [9], results from wind tunnel measurements show that fitting fins on the two leading sharp corners significantly improves the generated wind power by 150%. On the other hand, fitting fins on the two trailing corners reduces the output wind power. Also, fitting fins on all four corners leads to a minor improvement on the functioning of the harvester. Based on these observations, it was reported that fitting fins on all corners of a square cylinder significantly impacts aerodynamic characteristics of the square cylinder. This study [9] suggested that more benefit could be obtained by modifying the leading corners alone.

Tamura and Miyagi [17] carried out wind tunnel experiments to analyse the impacts of cylinder corner shapes and turbulence intensity on fluid dynamic forces on a square cylinder in two-dimensional and three-dimensional turbulent fluid flow. They reported that chamfered and rounded cylinder corner shapes cause drag reduction. Further, they observed that even at zero angle of attack, the windward edge primary separated flow reattaches to cylinder surface for a rounded corners cylinder. Letchford and Mason [18] carried out an experimental study on two full-size square cylinder sections with sharp and rounded corners in two different turbulent fluid flows. Research reported in [19] studied the impact of corner alterations in a two-dimensional turbulent flow around a square cylinder at an angle of attack. They reported that the average decrease in the drag coefficient of a square cylinder with modified corners was around 44.5 % for 6.5% turbulence intensity and round 41.5 % for 14 % turbulence intensity compared with the drag coefficient of an unmodified square cylinder.

Bearman et al. [20] reported the impacts of cylinder corner rounding on the fluid mechanics loads on square cylinders immersed in time-independent and oscillatory fluid flows. Their report stated that the drag force was very susceptible to the cylinder corner round forms when the incoming fluid flow was time-independent and to a larger amount for the case of oscillating flows too. Kawai [11] reported the impact of many corner alterations on the attributes of fluid flows past square cylindrical objects with rounded corners. He observed that, of the several changes assessed, the corner radius of the square cylinder provided the best choice for improving the fluid dynamic stability of the square cylinder through decrease of the resultant time-dependent fluid loads [11]. Tamura et al. [21] and Tamura and Miyagi [17] studied computationally and by experiments the impact of cylinder corner changes on the fluid mechanic loads. They reported a reduction in the wake size and in the mean values and rms values of the lift coefficient and the drag coefficient by around 10%. Dalton and Zheng [22], in a computational investigation of the uniform flow around a square cylinder and a diamond shaped cylinder with and without cylinder corner alterations, observed that rounding the cylinder corners provided an obvious decrease in the computed drag and lift coefficients. Miran and Sohn [23] computationally researched the impact of cylinder corner radius changes on the fluid flow around a square cylinder at a low Reynolds number of 500. They reported that the minimum value of the drag coefficient of the cylinder and the rms value of the lift coefficient of the cylinder happened at a ratio of corner radius to square height of about 0.2. Jaiman et al. [24] computationally investigated the result of rounded cylindrical corner on steady and freely oscillating square cylinders at Re values in the region of 100–200. They also reported that rounding of sharp corners defers the primary flow separation and also that the loads on the square cylinders showed a decrease in their values. Carassale et al. [12] reported the effect of corner modification on the fluid dynamic characteristics of square cylinders using wind tunnel experiments for two different corner round radius values and for the Reynolds number in the region of 17000 to 230000. They focused mainly on the investigation of the turbulent fluid flow behaviour in relation to the

angle of attack and reported that the rounding the corners causes to decrease the critical angle of attack for which the turbulent fluid flow reattaches on the side surfaces. Ajith Kumar et al. [25] using experiments studied the near wake region of a transversely vibrating square cylindrical section with various corner radius values employing the method of Particle Image Velocimetry (PIV) in a water channel. They concluded that increasing the corner radius reduces the chances for time-dependent instabilities of the square cylinder. Hu et al. [26] carried out experiments in the near wake region of square cylinders with various corner radius values using the methods of PIV, Laser Doppler Anemometry (LDA), and Hot-Wire Anemometry. Their conclusions included a statement that as the ratio of cylinder corner radius value to cylinder side length is increased from 0 to 0.5, the maximum intensity of the shed vortices was reduced. Nidhul[27] investigated the impact of corner shape on fluid flow behaviour for a flow past a two-dimensional square cylinder at a Reynolds number value of 150 and reported on the static pressure and also wall shear stress profiles on the square cylindrical wall. Delany and Sorensen [28] studied the variation of the drag coefficient of cylinders of different shapes with three different corner radius values at various Reynolds number. They observed that the drag coefficient reduced with increase in the cylinder corner radius. Predictions are presented [29] of the two-dimensional turbulent fluid flow past a square cylinder with rounded corners at the ranges of high Reynolds numbers. The impact of rounded corners on square cylinders has proven to be very difficult to predict with conventional turbulence closure models and the other results presented, supported the importance of capturing the impact of vortex shedding which are correctly accounted for by the turbulence closure models used. From the above review of most of the available research reports, it is observed that the corner radius and chamfer length effects were not studied by systematically modifying them. Also, it was observed that majority of the available research results presented experimental works. It is clearly observed from the above review that the impacts of corner alterations on the general fluid flow characteristics, and particularly very near the square cylinder, are very significant and evident in the shape of reduction in the mean fluid force values and fluctuating fluid forces values compared to the cylinders with sharp corners. It was also observed that most of the previous studies have been carried out for fluid flows at Reynolds number ranges that are far below of those Reynolds number ranges that are experienced in practice.

The aim of the present computational research is to add to the corpus of knowledge in this field. The concentration is on the computation of the turbulent fluid flows at high Re ranges past two-dimensional square cylinders whose corners are altered. The impacts of rounding the cylinder corners turn out to be very significant and not very easy to predict. This is due to, unlike in the case of fluid flow past a square cylinder with sharp corners, the position of the separation point here is not known and hence should be computed by correctly capturing the balance of the fluid forces of inertia, friction, and pressure. In this research, we concentrate on the more difficult problem where Re of the fluid flow is high and the flow is fully developed and turbulent. In the present study, Computational Fluid Dynamics technique is employed to study the turbulent fluid flow past square cylindrical geometries with and without corner alterations. The influence of leading corner modifications and trailing corner modifications have been studied separately.

2. Methods Computational Geometry Description

Figure 1 schematically shows a two-dimensional square cylinder in the computational domain. This two-dimensional computational domain is 2000mm long(L) and 1100mm wide(H). The height(D) of the basic square cylinder is 100mm. The air goes through the inlet plane of the duct from the left at a prescribed uniform speed. Computations have been carried out from the point of calculating the drag coefficient (C_D) on the cylinder with and without modifications. The Reynolds number based on the height of the basic square cylinder and inlet velocity was about 2.6x105. Effects of Reynolds number, and mesh size in the computational domain on the C_D have been studied for an unmodified square cylinder. Corner round radius (R) has been kept equal for all corners and similarly

chamfer length for chamfered corners has been kept equal for all corners. The symmetry of the modified configurations has been maintained. For chamfered corners, chamfering has been done at angle of 450 only for all corners. Figure 2 shows the modifications carried out at the corners of the square cylinder. Corner radius (R/D) and chamfer length (s/D) were gradually modified between 0 to 0.28.

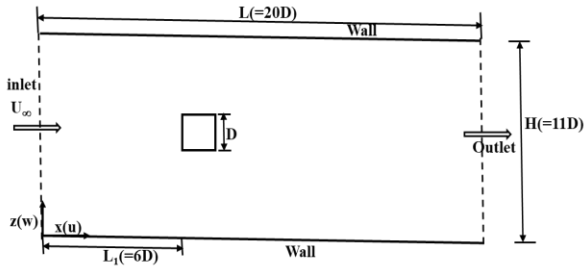

H=1100mm, L=2000mm, D=100mm, L1=600mm

Fig 1. Two-Dimensional square cylinder with sharp corners in the computational domain.

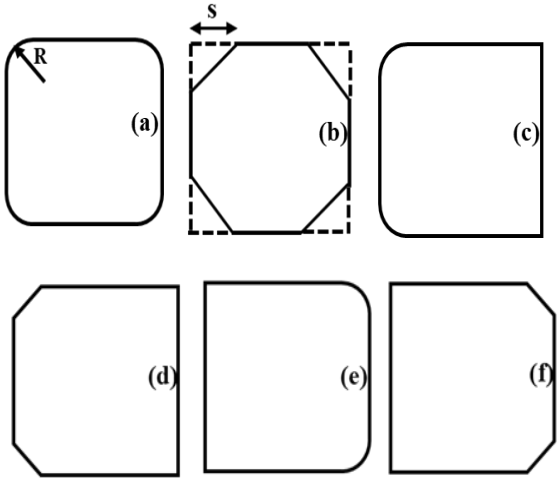

(a) All corners rounded with radius (R)
(b) All corners chamfered with length (s)
(b) Only leading corners rounded with radius (R)
(d) Only leading corners chamfered with length (s)
(e) Only trailing corners rounded with radius (R)
(f) Only trailing corners chamfered with length (s)

Fig 2. Two-Dimensional square cylinder with corner modifications.

3. Methods Computational Geometry Description

The transport equations, governing the fluid flow in the domain, are described using Cartesian coordinate system in which x and z coordinates will be taken as representing the independent variables.

3.1. Governing Equations

The flow was considered steady, two-dimensional, turbulent, single phase, incompressible, fully developed and of constant viscosity fluid. External applied body forces and buoyancy effects were neglected. Under these assumptions, Reynolds Averaged Navier-Stokes equations governing the mean flow development in the computational domain are given by [30-33]:

Horizontal component:

$$\frac{\partial}{\partial x}(\rho u^2)+\frac{\partial}{\partial z}(\rho uw)=\frac{\partial}{\partial x}\left(\Gamma\frac{\partial u}{\partial x}\right)+\frac{\partial}{\partial z}\left(\Gamma\frac{\partial u}{\partial z}\right)-\frac{\partial p}{\partial x}+\frac{\partial}{\partial x}\left(\Gamma\frac{\partial u}{\partial z}\right)+\frac{\partial}{\partial z}\left(\Gamma\frac{\partial u}{\partial x}\right)-\frac{2}{3}\frac{\partial}{\partial x}(\mathrm{div}\,\vec{V}) \quad (1)$$

Vertical Component:

$$\frac{\partial}{\partial x}(\rho uw)+\frac{\partial}{\partial z}(\rho w^2)=\frac{\partial}{\partial x}\left(\Gamma\frac{\partial w}{\partial x}\right)+\frac{\partial}{\partial z}\left(\Gamma\frac{\partial w}{\partial z}\right)-\frac{\partial p}{\partial z}+\frac{\partial}{\partial x}\left(\Gamma\frac{\partial w}{\partial z}\right)+\frac{\partial}{\partial z}\left(\Gamma\frac{\partial w}{\partial x}\right)-\frac{2}{3}\frac{\partial}{\partial z}(\mathrm{div}\vec{V}) \quad (2)$$

In the above equations, p [N/m2] is the pressure. The diffusion coefficient is defined by:

$$\Gamma=\mu+\mu\_\tau. \quad (3)$$

In which μ [Ns/m2] was the dynamics viscosity and μτ was the turbulent eddy viscosity.

The Equation of Continuity:

The mass conservation equation or the continuity equation, is given as follows:

$$\frac{\partial}{\partial x}(\rho u)+\frac{\partial}{\partial z}(\rho w)=0. \quad (4)$$

3.2. Turbulence Modelling

The flow variables of a turbulent fluid flow (velocity, pressure, etc.) exhibit fluctuations about an average value. The numerical computation of the instantaneous values is not economical with existing computing techniques and resources due to the high temporal and spatial frequencies that describe these flows and, hence, only the average values are calculated. EasyCFD [33] code implements two turbulence models, namely, the standard k-ε and Shear Stress Transport (SST) turbulence models. These two turbulence models are described below.

3.3. The Standard k-ε Turbulence Model

The standard construction of this turbulence model is illustrated in [33-36]. The turbulent eddy viscosity is defined as:

$$\mu_t = C_\mu \frac{\rho k^2}{\varepsilon} \quad (5)$$

The turbulence kinetic energy, k, and its rate of dissipation, ε[m^2/s^3], are calculated by solving two governing equations which are given as:

$$\frac{\partial}{\partial x}(\rho uk)+\frac{\partial}{\partial z}(\rho wk) = \frac{\partial}{\partial x}\left[\left(\mu + \frac{\mu_t}{\sigma_k}\right)\frac{\partial}{\partial x}\right] + \frac{\partial}{\partial z}[(\mu + \frac{\mu_t}{\sigma_k})\frac{\partial k}{\partial z}] + P_k - \rho\varepsilon \quad (6)$$

$$\frac{\partial}{\partial x}(\rho u\varepsilon) + \frac{\partial}{\partial z}(\rho w\varepsilon) = \frac{\partial}{\partial x}\left[\left(\mu + \frac{\mu_t}{\sigma_\varepsilon}\right)\frac{\partial \varepsilon}{\partial x}\right] + \frac{\partial}{\partial z}\left[\left(\mu + \frac{\mu_t}{\sigma_\varepsilon}\right)\frac{\partial \varepsilon}{\partial z}\right] + \frac{\varepsilon}{k}(C_1 P_k - C_2\rho\varepsilon \quad (7)$$

The term P_k is the rate of production of turbulent kinetic energy because of the mean velocity gradients:

3.4. The Shear Stress Transport (SST) Turbulence Model

The SST model characterizes a blend of the k-ε turbulence model and the k-ω turbulence model [37]. As per the study [38], the k-ε turbulence model is extra precise close to the rigid surface but exhibits an elevated-level of instability to the ω values in the undisturbed freestream zone, in which the k-ε turbulence model displays a improved performance. The SST turbulence model combines these two turbulence models, employing a weighting parameter calculated depending on the distance from the rigid surface.

The fluid flow governing transport equations in the computational domain are given as:

$$\frac{\partial}{\partial x}(\rho uk) + \frac{\partial}{\partial z}(\rho wk) = \frac{\partial}{\partial x}\left[(\mu + \sigma_k \mu_t)\frac{\partial k}{\partial x}\right] + \frac{\partial}{\partial z}[(\mu + \sigma_k \mu_t)\frac{\partial k}{\partial z}] + \overline{P_k} - \beta^*\rho\omega k \quad (10)$$

$$\frac{\partial}{\partial x}(\rho u\omega)+\frac{\partial}{\partial z}(\rho w\omega) = \frac{\partial}{\partial x}\left[(\mu + \sigma_\omega \mu_t)\frac{\partial \omega}{\partial x}\right] + \frac{\partial}{\partial z}[(\mu + \sigma_\omega \mu_t)\frac{\partial \omega}{\partial z}]+\frac{\overline{P_k}}{\nu_t}\alpha - \beta^*\rho\omega^2 + 2(1 - F_1)\rho\sigma_{\omega 2}\frac{1}{\omega}\left(\frac{\partial k}{\partial x}\frac{\partial \omega}{\partial x} + \frac{\partial k}{\partial z}\frac{\partial \omega}{\partial z}\right) \quad (11)$$

where ω is the dissipation rate of turbulent kinetic energy [s^{-1}]. The creation of turbulent kinetic energy is restricted to prevent the addition of turbulence in stagnant zones:

$$\overline{P_k} = \min(P_k, 10\beta^*\rho k\omega) \quad (12)$$

The weighting function Fl is presented by :

$$F_l = \tanh\left\{\left\{\min\left[\max\left(\frac{\sqrt{k}}{\beta^*\omega z}, \frac{500\nu}{z^2\omega}\right), \frac{4\rho\sigma_{\omega 2}k}{CD_{k\omega}z^2}\right]\right\}^4\right\} \quad (13)$$

And

$$CD_{k\omega} = \max\left[2\rho\sigma_{\omega 2}\frac{1}{\omega}\left(\frac{\partial k}{\partial x}\frac{\partial \omega}{\partial x} + \frac{\partial k}{\partial z}\frac{\partial \omega}{\partial z}\right), 10^{-10}\right] \quad (14)$$

in which z is the distance from the neighbouring rigid surface and ν is the kinematic laminar molecular viscosity. F_1 is equal to zero away from the rigid surface (k-ε turbulence model) and is modified to unit value in the boundary layer (k-ω turbulence model). The smooth change-over is done using the distance z. The turbulent eddy viscosity is calculated using the equation given below:

$$\nu_t = \frac{a_1 k}{\max(a_1\omega, SF_2)} \quad (15)$$

in which S was the invariant measure of the mean strain rate, defined by :

$$S = \sqrt{S_{ij}S_{ij}} \quad ; \quad S_{ij} = \frac{1}{2}\left(\frac{\partial u_i}{\partial x_j} + \frac{\partial u_j}{\partial x_i}\right) \quad (16)$$

And

$$F_2 = \tanh\left\{\left[\max\left(\frac{2\sqrt{k}}{\beta^*\omega z}, \frac{500\nu}{z^2\omega}\right)\right]^2\right\} \quad (17)$$

The constants of the turbulence model are calculated as a combination of the k-ε turbulence model and the k-ω turbulence model, through a general equation given

$$\alpha = F_1\alpha_1 + (1 - F_1)\alpha_2 \quad (18)$$

The other model constants are:

α_1=5/9, β_1=3/40, σ_{k1}=0.85, $\sigma_{\omega 1}$=0.5, α_2=0.44, β_2=0.0828, σ_{k2}=1.0, $\sigma_{\omega 2}$=0.856, β^*=0.09

The above set of governing equations have been solved, along with suitable boundary conditions for the computational domain, using numerical methods. The near wall treatment of momentum and turbulence equations as implemented in EasyCFD[33] obeys the suggestion explained in [39]. The basic notion behind the automatic wall

functions is to change from a low-Reynolds number scheme to a wall function built on the mesh nodes close to the wall. The first order upwind method was used to discretize the momentum equations, turbulent kinetic energy and turbulence dissipation rate equations. The Semi-Implicit Method for Pressure-Linked Equations-Consistent (SIMPLEC) method was implemented for the pressure velocity interactions[33,40]. At the inlet of the computational domain, a uniform velocity condition is given. The exit was considered as a pressure outlet. On the walls the zero mean velocity condition was imposed. The computational fluid dynamics software EasyCFD[33] was chosen to solve these equations because of its capability, simplicity and user-friendliness. This software uses a finite-volume based discretization method. The computations are converged when the normalized residues for continuity and momentum equations are less than 0.0001.

4. Results and Discussion

4.1. Validation of computational modelling

A two-dimensional computational domain has been constructed. The commercially available EasyCFD software [40] was used for construction of the geometry for the present computations. The computational methodology and present modelling were validated by using the following methods.

1. Comparing the present computational results with available results.
2. Carrying out grid independence study.
3. By checking mass flow at the inlet and outlet.

4.2. Grid independence analysis

A grid independence analysis was carried out in the computational domain to rule out the impact of the grid size (number of nodes in the computational domain. Also known as the mesh size) on the results. The calculations were carried out by employing the standard SST turbulence model. The drag coefficient (C_D) was kept as a parameter to evaluate the performance of various mesh sizes. The drag coefficient (C_D) of the cylinder was calculated as follows.

$$C_D = \text{Drag coefficient} = \frac{\text{Total Drag force on the cylinder}(F_D)}{0.5 \times \text{Density of the fluid} \times U_{in} \times U_{in} \times D} \quad (19)$$

Computations were conducted on the fluid flow past a rectangular cylinder of aspect ratio 5.

Table 1. The drag coefficient (CD) of an unmodified square cylinder with grid size.

Grid	C_D	% Difference
19880	1.9700	
21820	1.8780	**4.9**
23350	1.7942	**4.7**
24430	1.7400	**3.1**
25310	1.7047	**2.1**
30670	1.6720	**2.0**
32070	1.6640	**0.5**

Table 1 presents the results of the drag coefficient (C_D) for different grid sizes. From Table 1, it is seen that computations with grid sizes above 30670 nodes in the computational domain did not show any significant difference for the drag coefficient (C_D). Hence it was concluded to use a mesh size of about 32000 nodes for all computations.

4.3. Comparing the present computational results with previous result.

These preliminary computations of drag coefficient of square cylinder with sharp corners are compared with the computational results presented in the report[41]. From the study presented in the report[41], the drag coefficient for an unmodified square cylinder was 1.818 and 1.909 using k-ε turbulence model and SST turbulence model respectively. In the present study, at the same Reynold number, the drag coefficient of a square cylinder with sharp corners was 1.672 and 1.799 using k-ε turbulence model and SST turbulence model respectively. The difference in the drag coefficient values being about 8% and 5.8% using k-ε turbulence model and SST turbulence model respectively. The current study indicates that the presently computed and earlier computed results agree reasonably well.

4.3. By checking mass flow at the inlet and outlet.

The validation of present methodology was also carried out by monitoring the residuals during the computations and keeping balance of the mass flow at the inlet and outlet planes. The mass flow difference between the inlet and the exit planes is 0.001% which is very small.

4.4. Effect of Reynolds number on the drag of a square cylinder with sharp corners

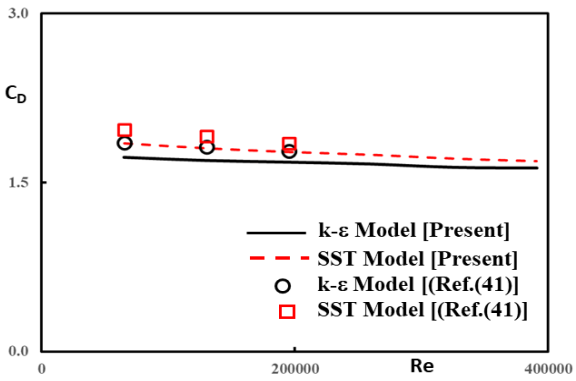

Fig. 3. Drag coefficient for a square cylinder with sharp corners with Reynolds number

In this section the results for the influence of Reynolds number on the drag coefficient (C_D) of a square cylinder with sharp corners are presented. The flow Reynolds number was calculated using the inlet velocity and the side length of the square cylinder. The inlet velocity was varied between 10 m/s to 60 m/s so that the Reynolds number varied from about 65000 to about 400000. Figure 3 gives the result for the variation of the drag coefficient (C_D) with the Reynolds number from the present computations and from a previous computational study [41]. From the results presented in the Fig. 3, it is seen that the drag coefficient (C_D) varies very slightly as the Reynolds number goes up and that the drag coefficient (C_D) tends to a constant value of 1.672 and 1.799 in the present study for k-ε and SST turbulence models respectively. This value of drag coefficient (C_D) closely matches with the experimental data given in the report [42] which was1.989 for the drag coefficient (C_D) of a square cylinder, with a deviation of about 14% and 9% using k-ε and SST turbulence models respectively. These differences in the C_D values may possibly be because present study was carried out in the two-dimensional computational domain and the experimental study [42] was carried out in three-dimensional flow. Also, it should be mentioned here that the previous computational study [41] presented in Fig. 3 was carried out in the Reynolds number range of 65000 to 200000. It can be observed, from the Fig. 3 that the same trend is obtained using both turbulence models in the present computational study.

4.6. Effect of modifying all corners

In this section the results of the effect of modifying all four corners of a square cylinder with sharp corner are presented and discussed. Figures 4 and 5 present the contour plots of streamwise component of mean velocity and the turbulent kinetic energy in the computational domain. Contour plots for all the configurations are not presented here to avoid cluttering and to enhance the clarity. However, the contour plots of streamwise component of mean velocity and turbulent kinetic energy are presented for three configurations, namely, the unmodified square cylinder, the modified cylinder with corner chamfer s/D=0.24 and the modified cylinder with corner radius R/D=0.24. These values for chamfer length and corner radius are chosen because the value of C_D starts increasing beyond this value of corner chamfer length and corner radius as can be seen later. Contour plots based on the computations using k-ε turbulence model only are presented here. Scales for these contour plots are provided below the contour plots.

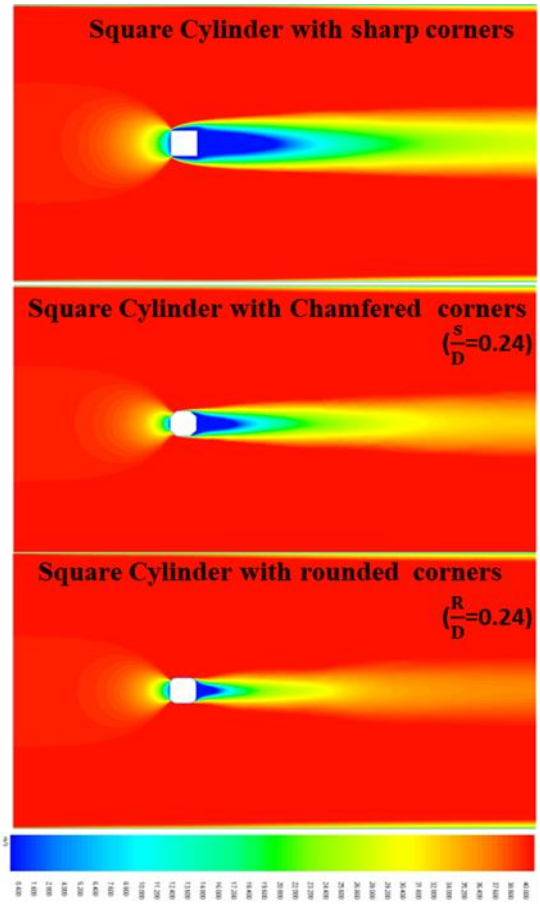

Fig. 4. Contour plot of x-component of mean velocity in the computational domain.

From Fig. 4, it can be seen clearly that the low velocity region behind the modified square cylinder with rounded corners is the smallest with the low velocity region behind the basic unmodified square cylinder being the largest. The size of the low velocity region behind the modified square cylinder with chamfered corner is in between the sizes of the regions behind unmodified square cylinder and the modified square cylinder with rounded corners.
From Fig. 4, it can be seen clearly that the low velocity region behind the modified square cylinder with rounded corners is the smallest with the low velocity region behind the basic unmodified square cylinder being the largest. The size of the low velocity region behind the modified square cylinder with chamfered corner is in between the sizes of the regions behind unmodified square cylinder and the modified square cylinder with rounded corners.

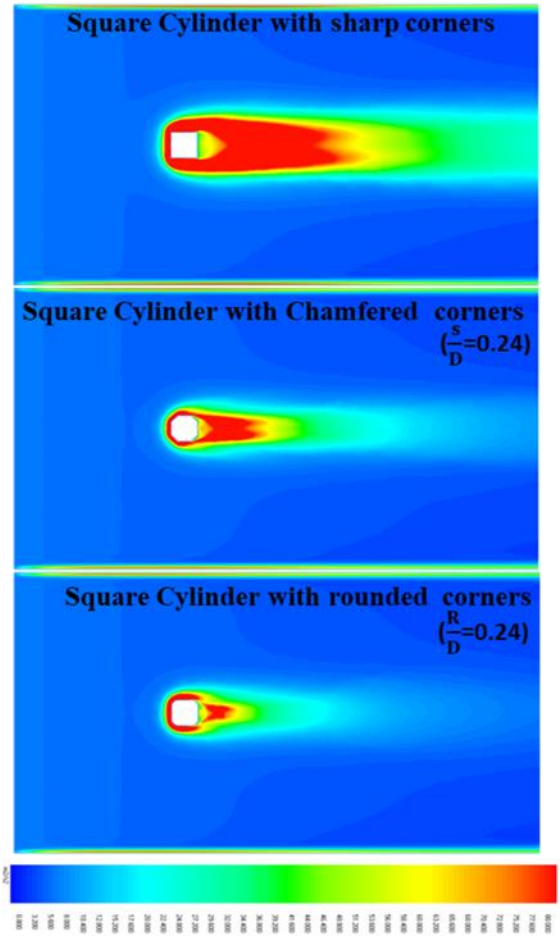

Fig. 5. Contour plot of turbulent kinetic energy in the computational domain.

From Fig. 5, it can be seen clearly that the modified square cylinder with rounded corners produced less amount of turbulent kinetic energy and hence the narrowest wake region of high turbulence compared to the unmodified square cylinder and modified square cylinder with chamfered corners. The unmodified square cylinder produced the largest high turbulence region around it. Figures 4 and 5 suggest that the modified square cylinder with rounded corners may be causing less disturbance to the flow as it may be experiencing less drag force.

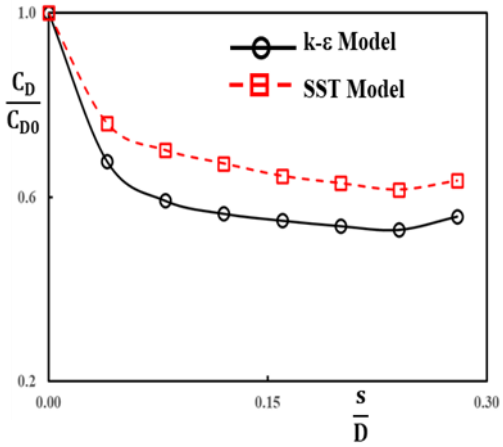

Fig. 6. Drag coefficient variation with corner chamfer length.

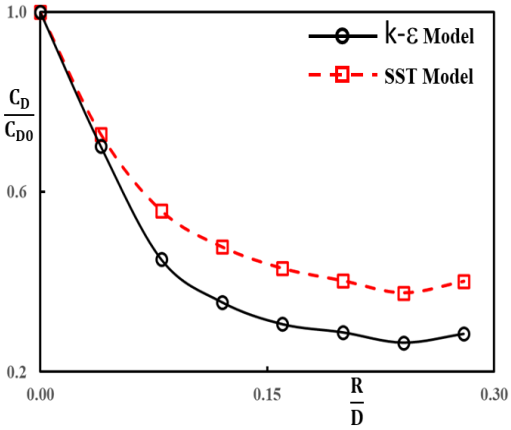

Fig. 7. Variation of drag coefficient with corner round radius.

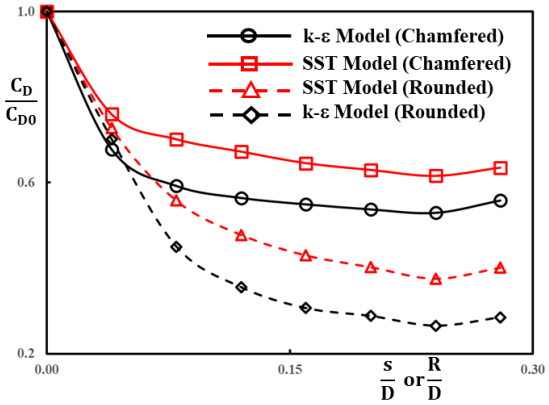

Fig. 8. Variation of drag coefficient with corner round radius and corner chamfer.

Figures 6-8 present the variation of drag coefficient (C_D) with chamfer length (s/D) or with corner radius (R/D). In these figures and in all subsequent figures, chamfer length (s) and corner radius (R) have been non-dimensionalised using the height of the unmodified square cylinder(D) whereas the drag coefficient C_D has been divided by C_{D0} which is the coefficient of drag for the unmodified basic square cylinder. From these figures it can be seen that the drag coefficient decreased with increase of chamfer length or corner radius up to a chamfer length of or up to a radius of 0.24D and beyond that length, the value of C_D started to increase. Also, from these figures it can be seen that the SST turbulence model predicts higher values for C_D than the k-ε turbulence model. From these graphs, it is seen that the lowest drag coefficient is achieved for the configurations with chamfer length of or a radius of 0.24D, and the configuration with corner radius of 0.24D gave the least drag coefficient. Because of this reason, the contour plots of streamwise component of mean velocity and turbulent kinetic energy were presented and discussed for the configurations with corner chamfer length and corner radius of 0.24D and more results in some of the following figures.

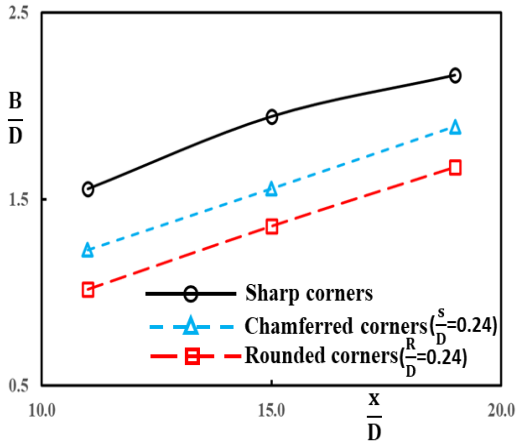

Fig. 9. Variation of wake half-width in the wake behind the square cylinder.

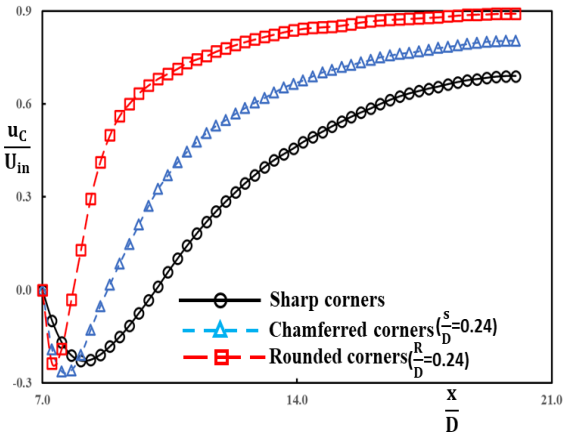

Fig. 10. Variation of centreline velocity in the wake behind the square cylinder.

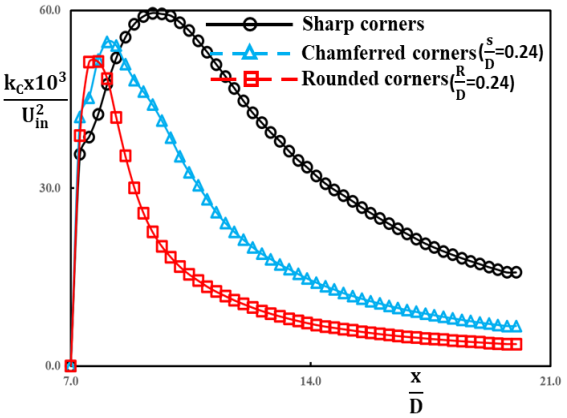

Fig. 11. Variation of turbulent kinetic energy along the centreline of the wake behind the square cylinder.

Figure 9 presents the variation of wake half-width(B) along the streamwise direction. Wake half-width is defined as the location in the z-direction where the difference between the local mean velocity and the undisturbed freestream velocity is exactly half of the difference between the undisturbed freestream velocity and the value of mean velocity on the centreline of the wake at the streamwise(x-direction) location. Wake half-width is calculated based on the streamwise component of mean velocity. Wake half-width(B) is non-dimensionalised using the height(D) of the unmodified square cylinder. It can be seen, from the Fig. 9, that wake half-width increased as the streamwise distance increased for all the configurations, as is to be expected. It is seen that the wake half-width being lower for the modified configurations. Since it is known that the size of the wake half-width is proportional to the drag experienced by the object, it can be inferred that chamfering and rounding the corners of the square

cylinder do provide drag reduction benefits. It is observed that the corner rounding results in the wake half-width becoming lower than other two configurations, inplying that rounding of corner yields the highest drag reduction benefits.

Figure 10 presents the variation of streamwise component of mean velocity values on the wake centreline(U_C) on the wake centreline along the streamwise direction. It is seen from the Fig. 10 that the wake centreline mean velocity increased as the streamwise distance increased for all the configurations as is to be expected. It is seen that the centreline mean velocity is higher for the modified configurations. Since it is known that the centreline velocity value depends on the width of the wake region and the width of the wake region is proportional to the drag experienced by the object, it can be inferred that chamfering and rounding the corners of the square cylinder do provide drag reduction benefits. It is also observed that, the corner rounding results in the centreline mean velocity becoming higher than other two configurations suggesting that rounding of corner yields the highest drag reduction benefits.

Figure 11 presents the variation of the turbulent kinetic energy(K_C) values on the wake centreline along the streamwise direction. It is seen from the Fig. 11 that, the values of turbulent kinetic energy on the wake centreline increased as the streamwise distance increased for all the configurations, as is to be expected. It is seen that the centreline turbulent kinetic energy is lower for the modified configurations. Since it is known that the turbulent kinetic energy production depends on the drag experienced by the object, it is suggested that chamfering and rounding the corners of the square cylinder do provide drag reduction benefits. It is also observed that, the corner rounding results in the turbulent kinetic energy on the wake centreline are lower than other two configurations inferring that rounding of corner yields the highest drag reduction benefits. The wake half-width, centreline mean velocity and the turbulent kinetic energy values on the wake centreline are presented in the wake region after the reattachment of the separation bubble behind the square cylinders.

Table 2. Reattachment length behind the square cylinder.

Square Cylinder	Reattachment length($\frac{S_L}{D}$)
Sharp corners	3.13
Chamfered corners ($\frac{s}{D}=$	1.80
Rounded corners ($\frac{R}{D}=$	0.86

Table 2 presents the reattachment length (SL) or size of the separation region behind the square cylinder configurations. From the Table 2, it is seen that reattachment length or separation region size behind the square cylinder with rounded corner is the smallest compared to other two configurations with basic square cylinder with sharp corners having the largest separation region behind it. Since the size of the separation region depends on the drag of the body, it can be inferred that the drag coefficient of the modified square cylinder with rounded corners is the lowest. This inference supports our previous arguments based on drag coefficient data and contour plot presentations.

4.7. Effect of modifying only leading corners

In this section the results of the impact of modifying only the leading corners of a square cylinder are presented and discussed. The trailing corners are left unmodified. In this section only drag coefficient results are presented. Figures 12-14 present the variation of drag coefficient (C_D) with chamfer length (s/D) or with corner radius (R/D). In these figures, chamfer length (s) and corner radius (R) have been non-dimensionalised using the height of the unmodified square cylinder(D) whereas the drag coefficient C_D has been divided by C_{D0} which is the drag coefficient of the unmodified square cylinder. From these figures it is seen that the drag coefficient decreases with increase in chamfer length or corner radius up to a chamfer length of or up to a radius of 0.24D and beyond that length, the value of C_D started to increase. Also, from these figures it is seen that the SST turbulence model predicted higher values for C_D than the k-ε turbulence model. From these graphs, it is seen that the lowest drag coefficient is achieved for the configurations with chamfer length of or a radius of 0.24D, and the configuration with corner radius of 0.24D gave the least drag coefficient. It is seen from these figures that the trend for the variation of drag

coefficient with chamfer length or corner radius is the same as the flow in which all corners of the square cylinder are modified presented earlier. Comparing the figures 6-8 and figures 12-14, it can be observed that most of the drag reduction benefits come from the modification of leading corners.

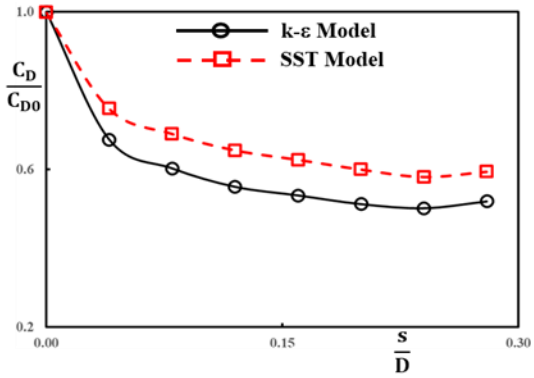

Fig. 12. Leading corners alone chamfered.

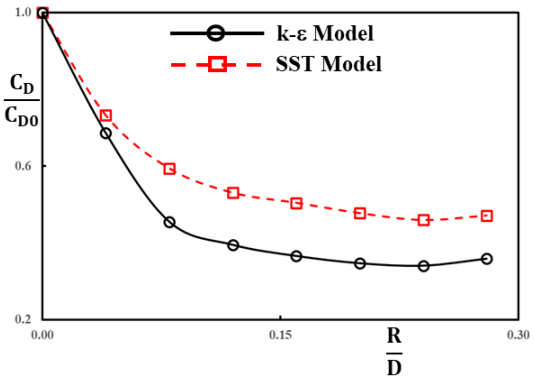

Fig. 13. Leading corners alone rounded.

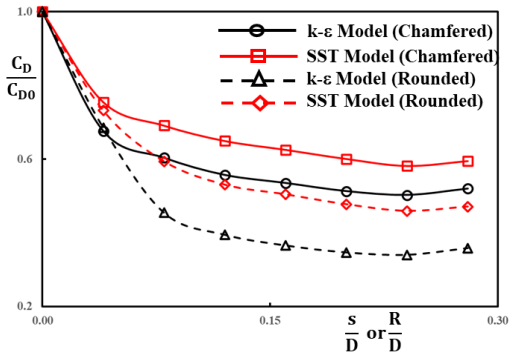

Fig. 14. Variation of drag coefficient with leading corners alone modified

4.8. Effect of modifying only trailing corners

In this section the results of the impact of modifying only the trailing corners of the square cylinder with sharp corners are presented and discussed. The leading corners are left unmodified. In this section only drag coefficient results are presented.

Figures 15-17 present the variation of drag coefficient (C_D) with chamfer length (s/D) or with corner radius (R/D). In these figures, chamfer length (s) and corner radius (R) have been non-dimensionalised using the height of the unmodified square cylinder(D) whereas the drag coefficient C_D has been divided by C_{D0} which is the drag coefficient of the unmodified square cylinder. From these figures it is seen that the drag coefficient, albeit slightly, increased with increase in chamfer length or corner radius. Also, from these figures it is seen that the SST turbulence model predicted higher values for C_D, though only slightly, than the k-ε turbulence model for all chamfer lengths and corner radius. Comparing the figures 6-8, figures 12-14 and figures 15-17, it is observed that most of the drag reduction benefits come from the modification of leading corners and, in fact, modifying the trailing corners alone contributes to an increase in drag.

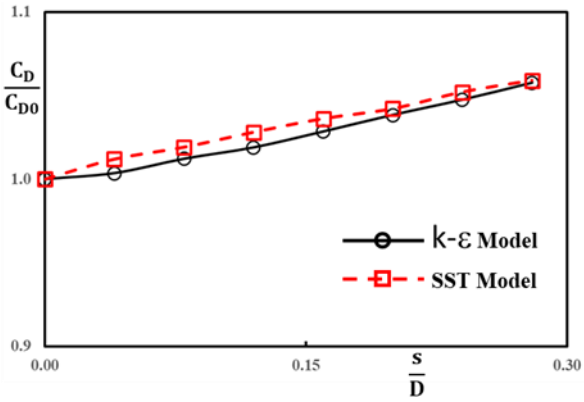

Fig. 15. Variation of drag coefficient with trailing corners alone chamfered.

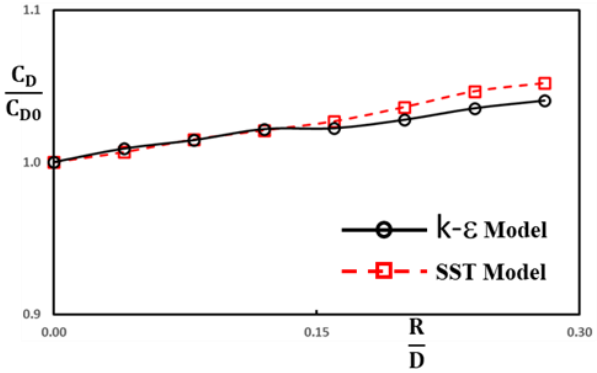

Fig. 16. Variation of drag coefficient with trailing corners alone rounded.

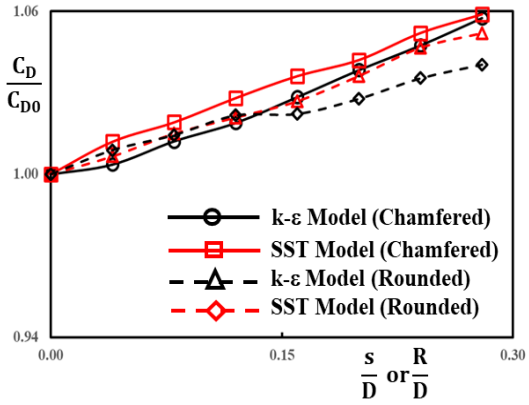

Fig. 17. Variation of drag coefficient with trailing corners alone modified.

Table 3. Drag reduction with corner modifications.

Turbulence Model	Drag Reduction			
	Chamfered corners		Rounded corners	
	All	Only leading	All	Only leading
k-ε	47%	50%	68%	70%
SST	39%	42%	64%	67%

Table 3 presents the results of reduction in drag coefficient achieved in the current study. This table presents the drag reduction data only for the configurations for which maximum drag reduction was achieved, namely a square cylinder with corner chamfer of 0.24D and a square cylinder with corner rounding radius of 0.24D. As it can be seen from the Table 3, maximum drag reduction is achieved when the corners are rounded, and k-ε turbulence model predicts maximum drag reduction. Also, it is seen from the Table 3 that modifying only the leading corners could give more benefit in drag reduction than, albeit slightly, modifying all corners. From the data given in Table 3, it can be inferred that modifying the trailing corners does not provide any drag reduction benefits and, in fact, it increases the drag, though slightly, as presented in the Figures 15-17.

5. Conclusions

In this research project, the drag coefficient of several configurations of a square cylinder with and without corner modifications, in a two-dimensional turbulent fluid flow was studied. Corner radius and chamfer length were gradually modified between 0 to 0.28D. The square cylinder with rounded corner radius of 0.24D had the lowest drag coefficient, which was followed by the square cylinder with a corner chamfer length of 0.24D, while the square cylinder with sharp corners had the highest drag coefficient.

The drag coefficient of a square cylinder decreases with corner adjustment. The greatest effect comes from rounded edges with a radius of 0.24D, causing a 68% decrease in the drag coefficient when compared to unmodified square cylinder. Chamfered corners, of chamfer length of 0.24D also cause a significant decrease of about 47% in the drag coefficient on the square cylinder, but being a straight edge, chamfer may be more suitable for engineering purposes. The flow patterns around the various geometries were significantly different, as revealed by the examination of the mean velocity and turbulence kinetic energy contours. The sharp-cornered square cylinder produced the most turbulence kinetic energy, which indicates that this unmodified square cylinder increases flow turbulence. The wake half width increases with streamwise distance for all the three cases. However, wake half-width is the lowest for the configuration with rounded corners. The mean velocity on the centreline in the wake decreases initially and then increases with streamwise distance for all the three cases. However, mean velocity on the centreline of the wake is the highest for the configuration with rounded corners. The values of turbulent kinetic energy on the centreline of the wake increases initially because of the turbulence generated by the body and then starts decreasing with streamwise distance for all the three cases. However, turbulent kinetic energy on the centreline of the wake is the lowest for the configuration with round corners. The reattachment length behind the square cylinder is the smallest for the square cylinder with rounded corners, followed by the square cylinder with chamfered corners, while the square cylinder with sharp corners had the highest reattachment length. The present study concludes that round corner cylinder has the narrowest wake while square

cylinder with sharp corners has the widest wake. The current computational study reveals that a large part of the drag reduction could be achieved by modifying the leading corners alone. The current study further reveals that the modification of trailing corners does not help in reducing the drag of the square cylinder. In fact, modification trailing corners leads to an increase in the drag of the square cylinder by a small quantity.

In conclusion, the round corner square cylinder may be aerodynamically more effective, and the shape of a square cylinder can have a considerable impact on its drag coefficient and fluid flow patterns. These results could help in the design of more effective fluid flow systems such as pipelines and channels and have considerable implications for fluid mechanics and engineering. These results could also help in the understanding of the effect of corner shape on the drag force affecting the aerodynamics of tall buildings, marine structures, road, and air-borne vehicles.

Refrences

[1] Abdelhamid T., Alam M. M., Islam M., (2021) Heat transfer and flow around cylinder: Effect of corner radius and Reynolds number. International Journal of Heat and Mass Transfer, 171, Article 121105. https://doi.org/10.1016/j.ijheatmasstransfer.2021.121105

[2] Bai H., Alam M. M., (2018) Dependence of square cylinder wake on Reynolds number. Physics of Fluids, 30, 015102

[3] Derakhshandeh J. F, Alam M. M., (2019) A review of bluff body wakes. Ocean Eng., Vol 182, Jun 2019, ISSN 0029-8018, https://doi.org/10. 1016 /j.oceaneng.2019.04.093 475-488

[4] Alam M. M., (2022) A review of cylinder corner effect on flow and heat transfer. Journal of Wind Engineering & Industrial Aerodynamics 229: 1-28, 105132, ISSN 0167-6105, https://doi.org/10. 1016/ j.jweia.2022.105132.

[5] Gao DL, Chen WL, Li H, Hu H (2017) Flow around a slotted circular cylinder at various angles of attack, Exp. Fluids 58: 1–15

[6] Tang H, Shum KM, Li Y (2019) Investigation of flutter performance of a twin-box bridge girder at large angles of attack, J. Wind Eng. Ind. Aerod., 186, 192–203. https://doi. org/10.1016/j.jweia. 2019.01.010.

[7] Xu Fu, Chen W. L., Xiao Y.Q., Li H., Ou J. P., (2014) Numerical study on the suppression of the vortex-induced vibration of an elastically mounted cylinder by a traveling wave wall. J. Fluids and Structures,44, 145–165. https://doi. org/10.1016/j. jfluidstructs.2013.10.005

[8] Chen W. L., Gao D. L., Yuan W. Y., Li H., Hu H., (2015) Passive jet control of flow around a circular cylinder. Exp. Fluids 56: 1–15

[9] Kwok KSC, Bailey PA (1987) Aerodynamic devices for tall buildings and structures, J. Eng. Mech., 113 (3), 1987, PP 349–365.https://doi.org/ 10.1061/ (ASCE)0733-9399(1987)113:3(349)

[10] Wang Q., Jiang Q., Hu G., Chen H., Li C., Xiao Y., (2021) Aerodynamic characteristics of a square cylinder with corner fins. Adv. Bridge Eng 2: 20-39

[11] Kawai H., (1998) Effect of corner modifications on aeroelastic instabilities of tall buildings. J. Wind Eng. Ind. Aerod., 74–76: 719-729. ISSN 0167-6105, https://doi.org/10.1016/ S0167-6105(98)00065-8

[12] Carassale L., Freda A., Marrè-Brunenghi M., (2014) Experimental investigation on the aerodynamic behaviour of square cylinders with rounded corners. J. Fluids and Structures 44: 195–204. https://doi.org/10.1016/j.jfluid structs.2013.10. 010.

[13] Zhang W., Samtaney R., (2016) Low-re flow past an isolated cylinder with rounded corners, Comp. Fluids, 136, 2016, 384–401. https://doi.org/10.1016/ j.compfluid.2016.06.025

[14] He G. S., Li N., Wang J. J., (2014) Drag reduction of square cylinders with cut-corners at the front edges, Exp. Fluids 55: 1–11

[15] Kurata M., Ueda Y., Kida T., Iguchi M., (2009) Drag reduction due to cut-corners at the front-edge of a rectangular cylinder with the length-to-breadth ratio being less than or equal to unity. J. Fluids Eng 131: 2–6

[16] Tse K. T, Hitchcock P. A., Kwok KCS, Thepmongkorn S, Chan C M (2009) Economic perspectives of aerodynamic treatments of square tall buildings. J. Wind Eng. Ind. Aerod., 97, (9-10), 455–467. https://doi.org/ 10. 1016 /j.jweia. 2009.07.005

[17] Tamura,T, Miyagi T (1999) The effect of turbulence on aerodynamic forces on a square cylinder with various corner shapes. J. Wind Eng. Ind. Aerod 83: 135-145

[18] Letchford, C., & Mason, M. (2011). Drag of square section tubes,13th Int Conf on Wind Eng., July 10-15, Amsterdam, Netherlands

[19] Mohamed I. K, Aissa W. A, (2016) Effect of corner modification on two-dimensional turbulent flow around a square cylinder with incidence J. Eng. Sciences, Assiut University, 44(1): 91–102

[20] Bearman P. W., Graham J. M. R., Obasaju E. D., Drossopoulos G. M., (1984) The Influence of Corner Radius on the Force Experienced by Cylindrical Bluff Bodies in Oscillatory Flow. App. Ocean Res 6(2): 83–89

[21] Tamura T., Miyagi T., Kitagishi T., (1998) Numerical Prediction of Unsteady Pressures on a Square Cylinder with Various Corner Shapes, J. Wind Eng. Ind. Aerod 74–76:531–542

[22] Dalton C., Zheng W., (2003) Numerical Solutions of a Viscous Uniform Approach Flow Past Square and Diamond Cylinders. J. Fluids and Struct 18 (3–4): 455–465

[23] Miran S., Sohn C. H., (2015) Numerical Study of the Rounded Corners Effect on Flow Past a Square Cylinder. Int. J.Num. Meth. in Heat Fluid Flow 25 (4)2015: 686–702

[24] Jaiman R. K., Sen S., Gurugubelli P. S., (2015) A Fully Implicit Combined Field Scheme for Freely Vibrating Square Cylinders With Sharp and Rounded Corners. Comp. Fluids 112: 1–18

[25] RAjith Kumar, Sohn C. H., Gowda B. H. L., (2009) Influence of Corner Radius on the Near Wake Structure of a Transversely Oscillating Square Column. J. Mech. Scie. Tech 23 (9): 2390–2416

[26] Hu J. C., Zhou Y., Dalton C., (2005) Effects of the Corner Radius on the Near Wake of a Square Prism. Exp. Fluids 40 (1): 106–118

[27] Nidhul K., (2014) Influence of Corner Geometry on the Flow Structure and Flow Characteristics for Flow Past a Square Column at Re 150. Int. J. Res. Aeron.Mech. Eng 2: 32–41

[28] Delany N. K., Sorensen N. E., (1953) Low Speed Drag of Cylinders of Various Shapes. National Advisory Committee for Aeronautics, Washington DC, Technical Note NACA-3038

[29] Dai S. S., Younis B.A., Zhang H. Y., Prediction of Turbulent Flow Around a Square Cylinder with Rounded Corners, J. Offshore Mech. Arctic E subsection Level 3

[30] Acheson D. J., (1990) Elementary Fluid Dynamics, Oxford Applied Mathematics and Computing Science Series, Oxford University Press ISBN 978-0-19-859679-0

[31] Batchelor G. K., (1967) An Introduction to Fluid Dynamics, Cambridge University Press ISBN 978-0-521-66396-0

[32] White F. M., (2006) Viscous Fluid Flow, McGraw-Hill ISBN 978-0-07-124493-0

[33] EasyCFD: A Two-dimensional Computational Fluid Dynamics software Manual Version 4.4.4, www.easycfd.net, 2020.

[34] Launder B. E., Spalding D. B., (1972) Mathematical Models of Turbulence. Academic Press London and New York, ISBN 0-12-438050-6

[35] Launder B. E., Spalding D. B., (1972) The Numerical Computation of Turbulent Flows. Comp. Meth. App. Mech.Eng 3: 269-289

[36] Djilali N., Gartshore I., Salcudean M., (1989) Calculation of Convective Heat Transfer in Recirculating Turbulent Flows Using Various Near- Wall Turbulence Models. Num. Heat Trans., Part A, 16: 189-212

[37] Patankar S. V., (1980) Numerical Heat Transfer and Fluid Flow, Hemisphere Publishing Corporation, Washington, D.C., ISBN 0-89116-522-3

[38] Menter F. R., (1983) Zonal two-equation k-□ turbulence model for aerodynamic flows, AIAA Paper 1993-2906

[39] Menter F. R, Kuntz M., Langtry R., (2003) Ten Years of Industrial Experience with the SST Turbulence Model, Turbulence, Heat and Mass Transfer 4, ed: K. Hanjalic, Y. Nagano, and M. Tummers, Begell House, Inc 625 – 632

[40] Menter FR et al. (2003) The SST Turbulence Model with Improved Wall Treatment for Heat Transfer Predictions in Gas Turbines, Proc. Int. Gas Turb. Cong., 2003 Tokyo, November 2-7

[41] Subaschandar N., (2022) Prediction of Turbulent Flow past a Rectangular Cylinder, J. Xi'an Univ. Arch.& Tech. (JXAT), China. Vol. XIV, Issue 1: 142-158. ISSN: 1006-7930

[42] Van J. P., Doormaal, Raithby G. D., (1984) Enhancements of the Simple Method for Predicting Incompressible Fluid Flows. Num. Heat Trans 7: 147-163